

Radiation Chemistry of Poly(methacrylates)

Abstract: An experimental study comparing radiation-induced degradation of poly(methacrylates) from ultraviolet, gamma-ray (^{60}Co), and electron-beam irradiation is presented. Analytical techniques used include mass spectroscopy, low-temperature electron paramagnetic resonance, and infrared spectrometry. The poly(methacrylate) polymers investigated are poly(methyl methacrylate) (PMMA), poly(*t*-butyl methacrylate) (PBMA), poly(methacrylic acid) (PMA), and poly(methacrylic anhydride) (PMA AN). All are shown to exhibit scission of the main chains and removal of the side groups when irradiated.

Introduction

Poly(methyl methacrylate), PMMA, widely used as an electron beam resist [1], has also been used as an x-ray resist [2]. An inherent part of the lithographic process in the fabrication of microcircuits is the degradation of the polymers due to ultraviolet light, x-rays, or electron-beam irradiation. The enhanced dissolution rate resulting from this degradation permits images to be developed on polymer films.

All poly(methacrylates) and their copolymers undergo main-chain scission when irradiated. Of these, PMMA has been one of the most favored polymers for studying gamma-ray-induced degradation. Many papers and review articles [3] have been published on its mechanism of degradation. However, few attempts have been made to correlate the various mechanisms that are associated with different kinds of irradiation. The purpose of our experiment is to study the degradation mechanisms of poly(methacrylates) resulting from three types of irradiation.

PMMA undergoes scission of the main chains and also removal of the side groups when irradiated. Evidence of this includes reduced molecular weight due to the main-chain scission [4], the characteristic electron paramagnetic resonance (epr) spectrum due to the macroradical generated by the main-chain scission [5], the epr spectra of methyl and formyl radicals formed by the removal of the side group [6], and the gaseous-product analysis derived mainly from removal of the side group [7]. For breakage of the main chain, interpretations include "hot radical" formation in the gamma-radiolysis [8], random scission for photodegradation below the glass transition temperature T_g [9], end-initiated depolymerization above T_g [10], and an "unzipping" mechanism above T_g [11].

Direct observation of intermediate species under various kinds of irradiation resulted in a unified view of the degradation process, revealing characteristics for each kind of radiation. In this study the polymer samples were exposed to ultraviolet light, gamma-rays, and electron beams. Analytical techniques include the application of mass spectroscopy to both positive and negative ions, low temperature Fourier transform and dispersive infrared spectrometry, and low-temperature epr spectroscopy. We report on the analysis of radiation-induced degradation, with particular emphasis on electron beams, of such poly(methacrylates) as poly(methyl methacrylate), PMMA; poly(*t*-butyl methacrylate), PBMA; poly(methacrylic acid), PMA; and poly(methacrylic anhydride), PMA AN, in powders and in thin films.

Experimental

• Materials

The atactic PMMA used for epr measurements in this study was a powder sample available from the E. I. Du Pont Company. However, for the mass spectroscopic study, the powder was dissolved in a solvent and cast onto a silicon or aluminum wafer to a thickness of about $1\ \mu\text{m}$ and then baked, under vacuum, at 60 to 80°C (333 to 353 K) for several hours to remove any trace of residual solvent. Syndiotactic and isotactic PMMA were prepared in this laboratory. PMA, PMA AN, and PBMA were obtained from Polyscience, Inc., Warrington, PA.

• Radiation sources

For uv-light irradiation, both medium- and low-pressure mercury lamps were used. Gamma-ray exposures were carried out at International Nutronics, Inc., Mt. View,

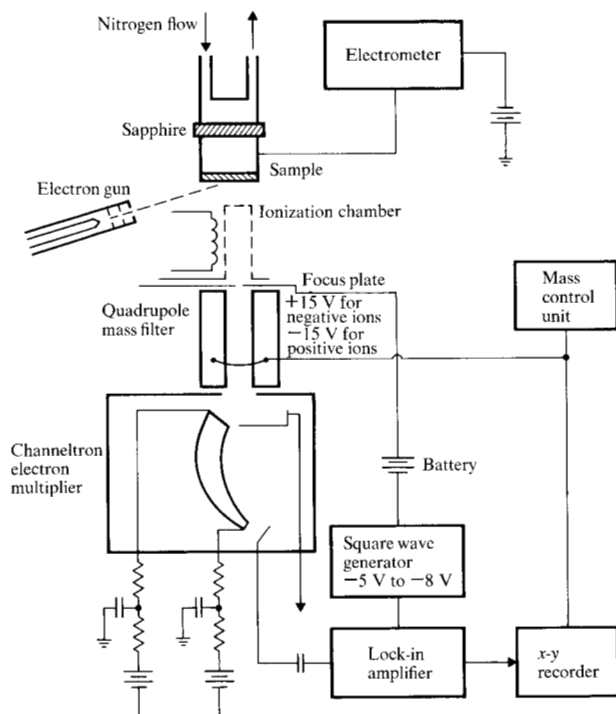


Figure 1 Mass spectrometric setup in modulation mode; the initial and the last stage potentials of the Channeltron were +500 V and +2200 V for negative ions, and -1700 V and grounded for positive ions.

CA. Electron-beam exposures were made with an Auger gun. Low energy (23 keV) electron exposures included an acceleration ring, whereas the high energy exposures (600 keV) were made by a Febetron Pulsar, via a thin aluminum foil window attached to a quartz sample tube.

• Spectroscopic measurements

Mass spectrometry Because of the fast adsorption of volatile products on a surface of the vacuum system, mass spectra of neutral and positive species were taken using oscilloscopic pictures in a field emission transistor amplifier mode. Negative ions were measured with a Uthe Technology International (UTI) mass analyzer modified to the modulation mode [12] shown in Fig. 1. Polymer films on an aluminum wafer, placed close to the ionization chamber of the mass spectrometer, were exposed to electrons with energies of about 100 eV from the ionization filament. Background measurements were taken with the sample "floated" at -150 V. With the sample grounded and the films exposed to the electrons, the resulting gaseous charged species were drawn into a hole in the focus plate, the potential of which was modulated by a square wave generator. A field of 500 V was applied to the entrance of the electron multiplier and therefore only negatively charged species could reach its initial opening. The secondary electrons generated were

accelerated to the last stage to which a field of 2200 V was applied. The same modulation technique was used for positive ions except that the polarity of the focus plate was reversed, and a negative voltage was applied to the entrance of the Channeltron.

EPR spectrometry A spectrometer operating in the X band was used for epr measurements.

Low temperature infrared spectrometry A Fourier transform infrared spectrometer was used to measure electron-beam-induced reactions, and a dispersive spectrometer was used for photochemical reactions. A stainless steel infrared cell, for electron beam exposures, was equipped with a high vacuum valve, potassium bromide windows, a liquid nitrogen Dewar, and an Auger gun, attached to the body at an angle of 45° to the polymer films. The polymer films were supported on a 100- μ m mesh copper screen, which was attached to a copper sample holder at the bottom of the Dewar. Because of the small change induced by electron exposures, 400 scans were usually taken for each run. (The photochemical experimental method has been described elsewhere [13].)

Visible emission spectroscopy Emission spectra during electron beam exposures were recorded on films with a half-meter spectrometer, through a quartz window.

• Analysis of gaseous products

Gaseous products, except hydrogen and methane, were separated with a gas chromatograph with a 2.4-m Ucon oil column and identified in comparison with authentic samples with respect to their mass, infrared (ir), and nuclear magnetic resonance (nmr) spectra.

Results

• Gaseous products

The yields of gaseous products formed from PMMA under various kinds of irradiation are shown in Table 1. The main difference between electron-beam exposure and uv and gamma-ray irradiation is the relatively high yield of hydrogen from the former. At elevated temperatures near 373 K, monomeric compounds such as methyl methacrylate, methyl pivalate, and methyl isobutyrate were also formed. During electron beam exposures of 2.5 keV at 297 K, the parent peaks of $\text{CH}_3\cdot$, $\text{CHO}\cdot$, and $\text{CH}_3\text{O}\cdot$ exceed those of their respective final products, CH_4 , CH_2O , and CH_3OH . This was so even after taking their fragmentation into account, which indicated that they were eliminated as radicals rather than as molecular species. The volatile products from PBMA in the radiolysis also show results similar to those obtained for PMMA [14]. Table 2 presents the yields of gaseous

Table 1 Efficiency of radiation in releasing gaseous products from poly(methyl methacrylate).

| Product | Quantum efficiency of uv photolysis at 254 nm (percent) | | <i>G</i> of ⁶⁰ Co γ-ray radiolysis (molecules/100 eV) | <i>G</i> of electron-beam exposure (molecules/100 eV) | | |
|---|--|-------------------|--|--|------|------|
| | | | | Energy (keV) | | |
| | 297 | 371 | 303 | 0.025 | 2.5 | 15 |
| | Temperature (K) | | | | | |
| | 297 | 371 | 303 | 383 | 297 | 371 |
| H ₂ | 0.3 | n.m. ^a | 0.1 ₃ | n.m. | 1.4 | 8.1 |
| CH ₃ · + CH ₄ ^b | 0.8 | n.m. | 0.5 | n.m. | 0.6 | 4.4 |
| CO | 0.7 | n.m. | 1.3 | n.m. | 1.2 | 2.5 |
| CHO | n.m. | n.m. | n.m. | n.m. | 0.3 | n.m. |
| CH ₃ O· + CH ₃ OH ^c | 0.9 | none | 0.03 | 0.01 | 0.4 | none |
| CH ₃ CH=CH ₂ | none | none | none | 0.08 | none | none |
| CO ₂ | 0.8 | 1.8 | 1.1 | 0.18 | 0.5 | 3.5 |
| (CH ₃) ₂ C=CH ₂ | none | 0.67 | none | 0.08 | none | none |
| HCOOCH ₃ | 0.8 | 0.13 | 0.01 | 0.004 | none | 1.13 |
| (CH ₃) ₂ CHCO ₂ CH ₃ | none | none | none | 0.02 | none | none |
| (CH ₃) ₃ CO ₂ CH ₃ | none | none | none | 0.01 | none | none |
| CH ₃ C(=CH ₂)CO ₂ CH ₃ | none | trace | none | 0.22 | none | 0.71 |
| M ⁿ /M ₀ ⁿ | n.m. | 0.45 | n.m. | 0.79 | n.m. | n.m. |

^an.m.: not measured.^bThe radical peaks exceed the parent peaks in the electron-beam exposure.^cA Hamill-type reactor (*J. Phys. Chem.* **74**, 1883 (1970)) was used.**Table 2** Efficiency of radiation in releasing gaseous products from poly(methacrylic anhydride) and poly(methacrylic acid) at 297 K.

| Product | Anhydride | | | Acid | |
|-----------------|--|--|--|--|--|
| | Quantum efficiency of uv photolysis at 254 nm (percent) | <i>G</i> of ⁶⁰ Co γ-ray radiolysis (molecules/100 eV) | <i>G</i> of electron-beam exposure at 2.5 keV (molecules/100 eV) | <i>G</i> of ⁶⁰ Co γ-ray radiolysis (molecules/100 eV) | <i>G</i> of electron-beam exposure at 2.5 keV (molecules/100 eV) |
| H ₂ | 0.06 | 0.05 | 4.7 | 0.08 | 4.6 |
| CH ₄ | 0.3 | 0.03 | 0.9 | 0.2 | 1.5 |
| CO | 2.2 | 4.2 | 9 | 2.9 | 3.5 |
| CO ₂ | 2.2 | 6.5 | 7 | 3.1 | 3.9 |

products from PMA AN and PMA under various kinds of irradiation. The major gaseous products from PMA AN and PMA in both uv-photolysis and gamma-radiolysis are CO and CO₂. In electron-beam exposures, however, hydrogen in addition to CO and CO₂ became one of the major products. The *G* values (number of chemical events produced per 100 eV of absorbed radiation) for the removal of the side groups under electron-beam exposures of 2.5 keV at 297 K are 2.0, 7.4, and 16 for PMMA, PMA, and PMA AN, respectively, because only the side groups are sources of CO, CO₂, and HCO.

• Ionic species

The positive ions observed during electron-beam exposures of PMMA at 2.5 keV at 297 K were CH₃⁺, CO⁺, CO₂⁺, CHO⁺, and CH₃O⁺; the ratios of their yields to those of the neutral species range from 10⁻³ to 10⁻⁴. This small observed yield, measured with the mass spectrometer, does not imply a small yield of positive macroions, which never leave the polymer films during electron-beam exposure. For PMA AN, the yield of gaseous positive ions was too small to be significant even in comparison with that from PMMA. The only major negative ions found from PMMA and PMA AN, during

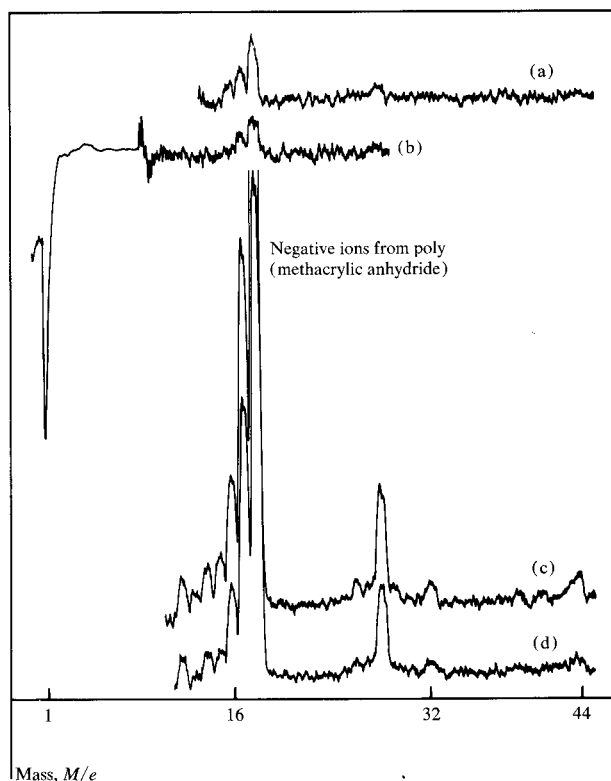


Figure 2 Typical negative ion mass spectrum of PMA AN; electron energy 70 eV. (a) Electron emission 0.5 mA, substrate grounded. (b) Overall, half the sensitivity shown in (a), and sensitivity below $M/e = 8$ is 1/20 that above 8. (c) Same as (a) except electron emission 2.5 mA. (d) Same as (a) except substrate "floated" at -150 V.

electron-beam exposures of about 100 eV, were negative hydrogen atoms, as shown in Fig. 2. However, small amounts of O^- , HO^- , H_2O^- , CO^- , O_2^- , and CO_2^- were identified from the PMA AN. The peak intensity of the negative hydrogen atoms was of a magnitude similar to that for the major neutral product, carbon monoxide. We do not know the absolute values for the ionization efficiencies of the neutral products or the probability of the charge loss of the negative hydrogen atoms. If we assume a fraction for the ionization efficiency of the carbon monoxide formed, and no charge loss, each 100-eV electron produces about one carbon monoxide molecule. Therefore, a fraction of its charge is lost to negative hydrogen atoms. In a typical electron-beam exposure of 100 eV, with an ionizing current of 5×10^{-4} A, a steady transmitting current of 7.2×10^{-6} A was observed through the polymer films. In exposures of a few keV energy, the formation of negative hydrogen atoms was observed. Because of a large gap between the film and the focus plate in this case, no quantitative measurement was carried out. To determine the effect of water in the

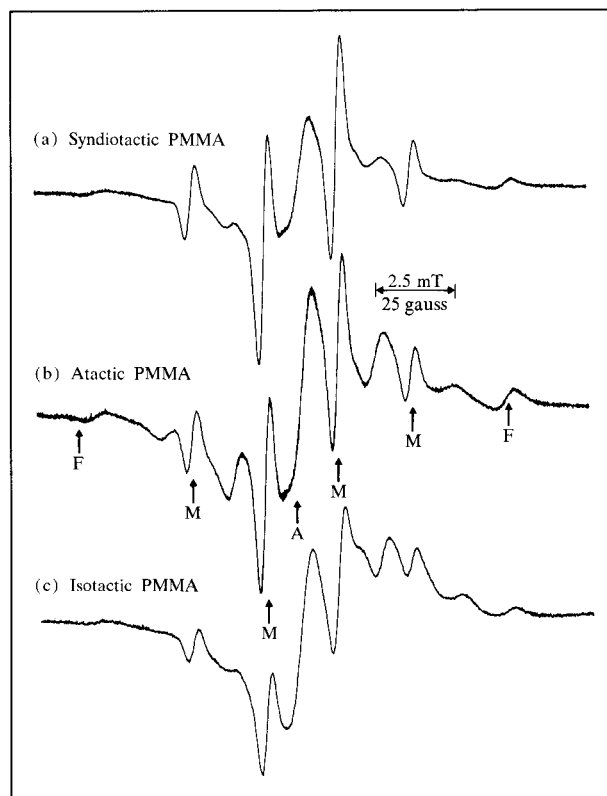


Figure 3 Effect of tacticity on the epr spectrum of PMMA under uv irradiation.

films on the formation of the negative hydrogen atoms, films of PMA cast on an aluminum wafer were treated at about 353 K with a vapor of deuterated water (D_2O). They were then baked at 463 K. PMA AN prepared in this way also yielded large numbers of negative hydrogen atoms, but only a very small number of D^- ions in less than a few percent of H^- .

During electron-beam exposures of energies higher than 1 keV, the intense blue emission, with its maximum at 435 nm, was observed from all poly(methacrylates). It became brighter at higher energies, but its intensity rapidly diminished when the electron beam remained in one spot. This luminescence was not a fluorescence but a delayed emission due to electron recombination with macro-cations [15].

• EPR study

UV photolysis The epr spectrum of PMMA at 77 K, after uv irradiation for several hours at that temperature, consisted mainly of four radicals (Fig. 3): $CH_3\cdot$ [four

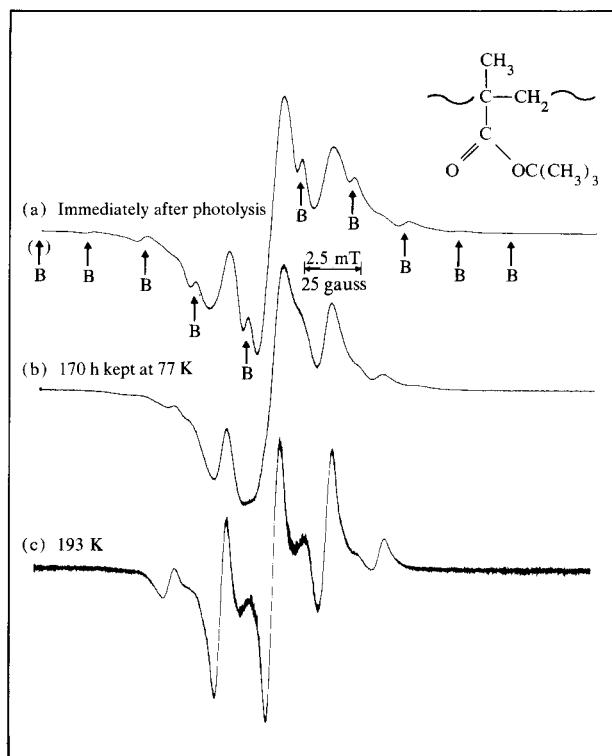


Figure 4 EPR spectrum of poly(*t*-butyl methacrylate) under uv irradiation at 77 K.

lines indicated by M, 23 gauss (2.3 mT) apart]; CHO· [two lines indicated by F, 110 gauss (11 mT) apart]; CH₃OCO· (one central, asymmetrical line indicated by A, with spectroscopic splitting factor $g = 2$); and (CH₃)₂C·CO₂CH₃ (a major part of the remaining seven-line signal). In addition to these radicals, a small amount of the propagating radical was found superimposed on the septet spectrum. The effect of tacticity on the epr spectrum is also shown in Fig. 3, which clearly indicates that the methyl radicals were the major radical species (35 percent of all radicals) in syndiotactic PMMA. However, in isotactic PMMA, the concentration of methyl radicals relative to all other radicals amounted to only 13 percent, and in atactic PMMA, the concentration amounted to 20 percent under uv irradiation at 77 K. When warmed up, the methyl radicals disappeared first, with the rate constants $0.9 \times 10^{-2} \text{ h}^{-1}$, $1.8 \times 10^{-2} \text{ h}^{-1}$, and $3.2 \times 10^{-2} \text{ h}^{-1}$ at 77 K for syndiotactic, atactic, and isotactic PMMA, respectively. Formyl and CH₃OCO· radicals disappeared next. The septet spectrum changed to the well known 5+4 line spectrum, which is fairly stable at room temperature in a vacuum [5, 6]. The septet spectrum became clearer in the epr spectra of PBMA, Fig. 4(b), and PMA AN, Fig. 5(a); it is completely free of other signals when the monomeric methacrylates, such as methyl methacrylate, sodium methacrylate, or methacrylic anhydride, are irradiated at 77 K without

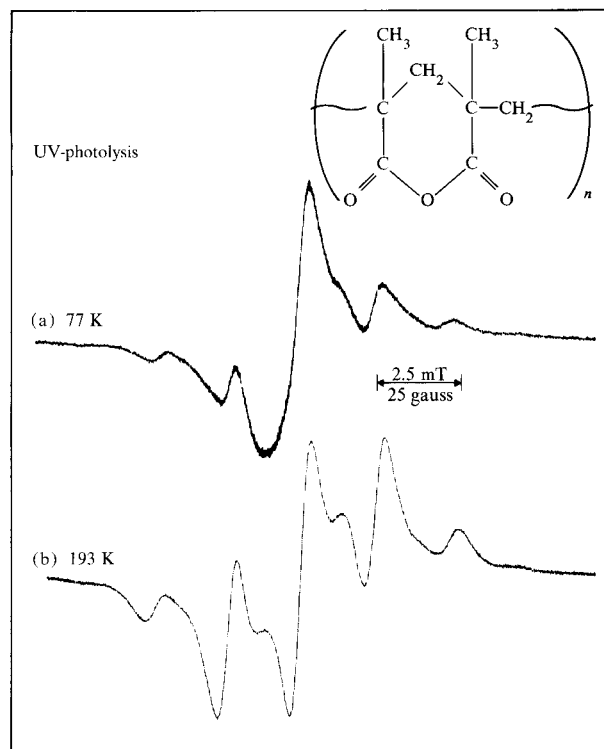
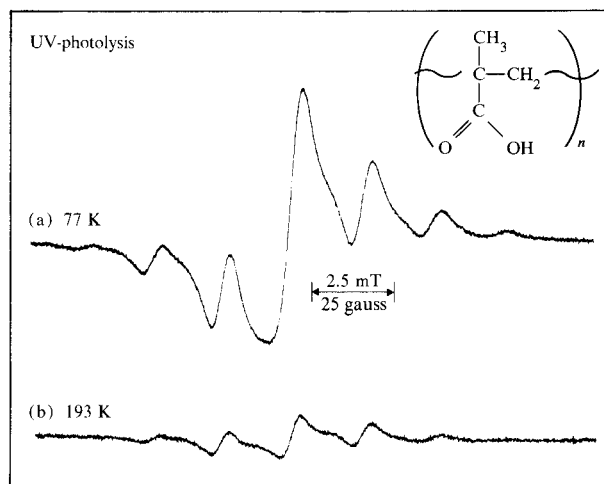


Figure 5 EPR spectrum of PMA AN exposed to uv irradiation at 77 K.

any polymerization initiator [16]. When PBMA was irradiated, *t*-butyl radicals [10 lines indicated by B, 22 gauss (2.2 mT) apart], Fig. 4(a), disappeared first with a rate constant $9 \times 10^{-2} \text{ h}^{-1}$ at 77 K, yielding the rather stable septet spectrum, which had a slightly larger line separation of 21.7 gauss (2.17 mT) than those observed in the PMA irradiated with a coupling constant of 20.2 gauss (2.02 mT), Fig. 6.

Figure 6 EPR spectrum of PMA exposed to uv irradiation at 77 K.



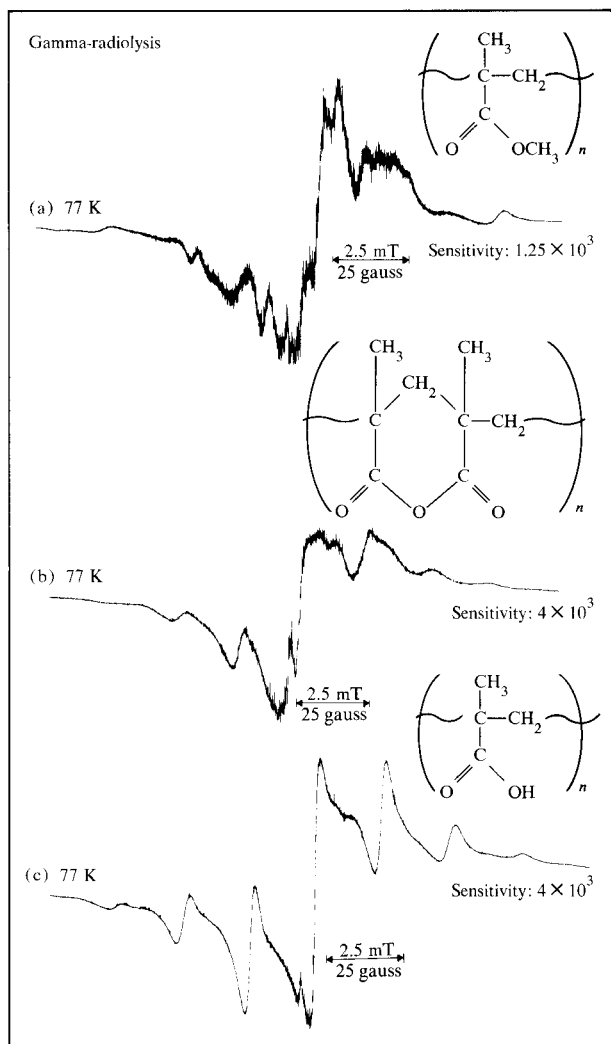


Figure 7 EPR spectra of poly(methacrylates) under γ irradiation at 77 K.

Gamma-ray radiolysis The energy input in the gamma-ray radiolysis is much higher than in the uv photolysis. This leads to the further decomposition of the acyl radicals. There is also direct hydrogen elimination from the side methyl as well as from the methyl ester, and possibly from the methylene group. The resulting epr spectrum, Fig. 7, is much more complex than those obtained after the uv photolysis. The main difference between PMA AN on one hand, and PMA and PMMA on the other, is the yield of free radicals, particularly the propagating radicals. The epr spectra of Fig. 6 were all taken under the same conditions, i.e., four Mrad, except for the sensitivity level as indicated. Even after taking the packing density of the powders into account, the yield of propagating radicals of PMA AN is two-thirds that of PMMA, and one-third that of PMA (although for the former the yields of gaseous products are much higher

than those of PMA and PMMA). This yield is related to the relative significance of the different reaction paths, that is, to the relative rates of the molecular and free radical fragmentation of the main chain, which are discussed in the following section.

Electron beam exposures High-energy electron pulses (600 keV, 10 pulses, 10 J each) at 77 K yielded an epr spectrum similar to the gamma-ray radiolysis spectrum, except for its central part ($g = 2.0$), as shown in Fig. 8. The yield of the radicals is not linear as a function of either the dosage or the number of pulses. When starting with photochemically generated propagating radicals, the radical concentration can be significantly reduced upon subsequent electron-beam exposure, as shown in Fig. 9. On the other hand, low-energy electron-beam exposure below 23 keV produces radicals inefficiently in comparison with high-energy electrons or gamma-ray radiation of comparable dosage. When the PMMA, already having a high concentration of photochemically generated radicals, was exposed to low-energy electrons, the concentration of the radicals diminished rather than increased, as shown in Fig. 10.

• *Low-temperature infrared absorption study*

The photochemical formation of a ketene end group from PMA AN has already been reported [13]. Differing from the photochemical reaction, the electron-beam exposures of 2.5 keV generated a small amount of the ketene end group but a large yield of carbon dioxide, as shown in the Fourier transform infrared spectrum of Fig. 11. This difference between uv photolysis and electron-beam exposure has been interpreted in terms of high-energy input in the electron-beam exposure rather than in the difference between the primary reactions, which is discussed in following sections.

Discussion

• *Poly(methyl methacrylate) and poly(*t*-butyl methacrylate)*

The large yield of methyl radicals in comparison with the propagating radicals, shown in Fig. 3, clearly indicates that a random main chain scission does not take place in the PMMA under uv irradiation; however, the main chain scission is induced by the ester side group elimination. Methyl radicals are unlikely to be eliminated from the tertiary position of the main chain, but they do arise from the disproportionation of $\cdot\text{COOCH}_3$, as reported for gamma-radiolysis [3, 7]. This claim is also supported by our results for PMA AN, where there was no indication of any formation of methyl radicals.

Formyl radicals also arise from $\text{O}\dot{\text{C}}\text{OCH}_3$, as is evidenced by its absence in the products of PMA AN and

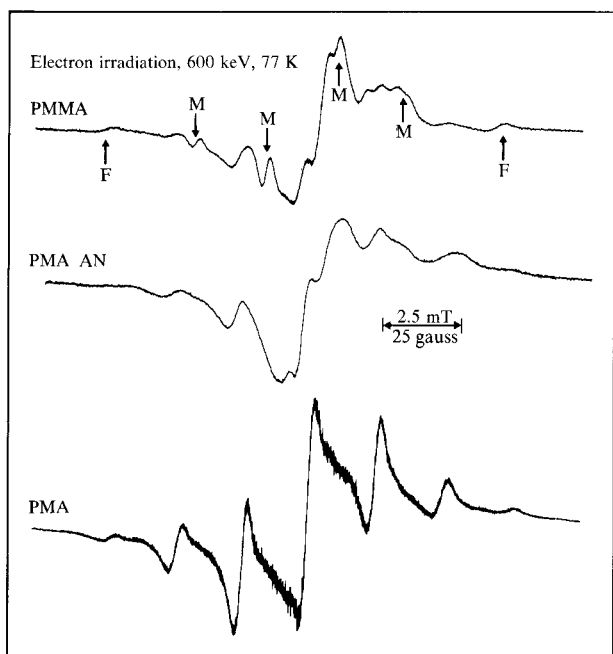


Figure 8 High-energy electron-beam irradiation (600 keV, 10 pulses, ≈ 100 J) at 77 K.

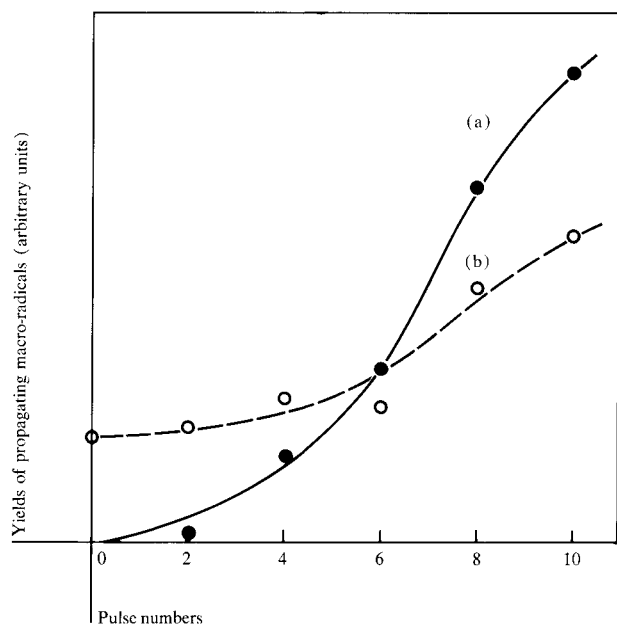


Figure 9 Effect of high-energy electron-beam irradiation on the yield of macro-radical (5+4 lines) from PMMA. (a) No preceding treatment; (b) uv irradiation before electron-beam exposure.

PBMA. A significant yield of HCOOCH_3 in uv photolysis is the most marked difference when compared to gamma-radiolysis. The former gives rise to a large ratio of side chain over main chain scission. Formation of methyl formate may be initiated by a process similar to

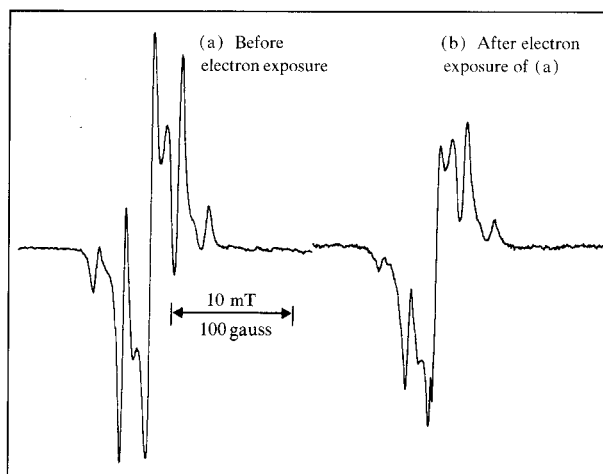


Figure 10 Twenty-three keV electron-beam exposure at low temperature for 2 h with 10 mA emission.

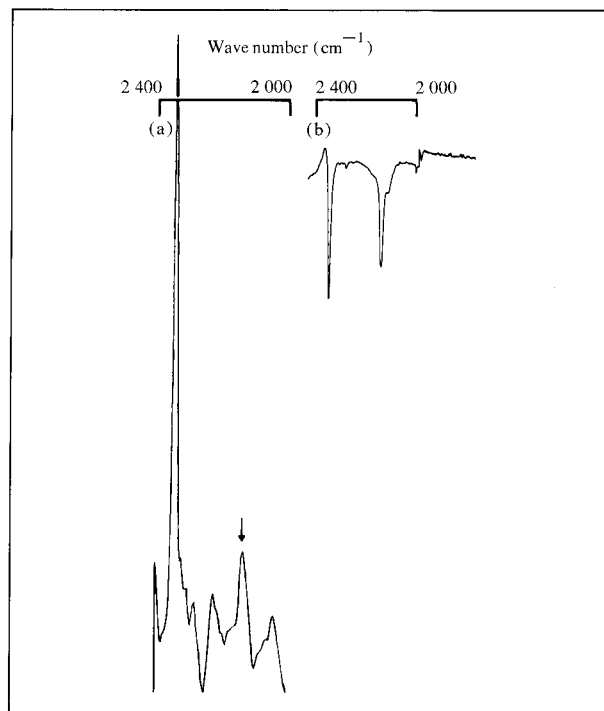
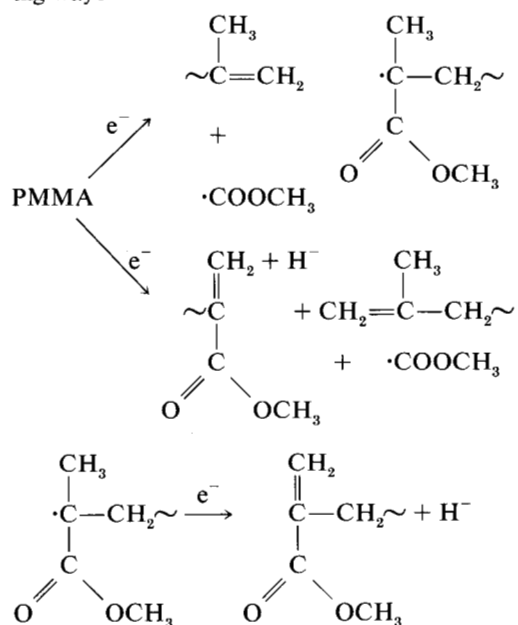


Figure 11 Low-temperature infrared spectra of PMA AN after irradiation; arrows indicate the ketene band. (a) Change of Fourier transform infrared absorption spectrum by electron-beam exposure of 10^{-3}C/cm^2 at 2.5 keV at 77 K. (b) Change of transmission spectrum by uv irradiation at about 170 K.

the Norrish type II reaction [17]. However, in gamma-radiolysis, positive PMMA ions formed via the Compton effect do not have photo-excited carbonyl groups to abstract the hydrogen atom. As shown in Table 1, the yield of hydrogen during gamma-radiolysis is the lowest

among the three kinds of radiation. The highest yield of hydrogen formation (Table 1) is found in low-energy electron-beam exposures. This is the most characteristic feature of electron-beam-induced degradation as opposed to degradation resulting from other sources of radiation. The reason for this high hydrogen yield appears to be the high electron affinity of the free radicals [18]. Thus, low-energy electrons, which are abundantly present in low-energy electron-beam exposures, attach to radicals yielding negative hydrogen atoms in the following ways:



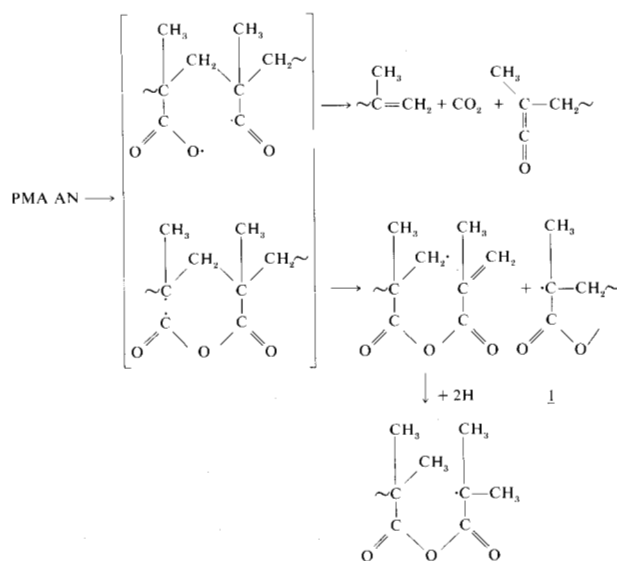
The negative hydrogen atoms may lose the charge on the wall surface, yielding hydrogen atoms and, eventually, hydrogen molecules. This explains the large yield of hydrogen atoms and molecules found in the low-energy electron exposures. The recombination of low-energy electrons with radicals conveniently explains a low yield of the propagating radical, and even its diminished yield under electron-beam exposure, as shown in Fig. 10. Figure 9 shows the photo-products including intermediates acting as retarders against formation of the propagating radical in high-energy electron-beam exposures [19]. Indeed, there are many secondary electrons with energies higher than the appearance potential for H^- , which is, for instance, 9.5 eV from ethane [20]. Thus, more than 31 percent of the secondary electrons generated by the 1-keV primary electrons have energies higher than 13 eV [21]. These electrons can directly eliminate negative hydrogen atoms and thereby generate hydrogen atoms from both methyl and methyl ester groups as shown in the above scheme. This appears to be the main reason for the complication of the epr spectra of PMMA observed after high-energy electron-beam exposures, Fig. 8, and gamma-ray irradiation, Fig. 7. Direct hydrogen

elimination from the methyl group attaching to the main chain is supported by the similarity of the epr spectra of PMA AN and PMMA under gamma-ray as well as high-energy electron-beam exposures. Another feature of the epr spectra of PMMA under gamma-ray and electron-beam exposures, as opposed to uv photolysis, was the increased decomposition of the $\text{CH}_3\text{OCO}\cdot$ radicals.

Poly(*t*-butyl methacrylate) undergoes main chain scission in the same manner as PMMA with the same propagating radical spectrum appearing (Fig. 4). The main difference is the yield of macro-radicals, which is five times higher for PBMA than for PMMA, indicating more strain in the main chain due to the bulky *t*-butyl ester group.

• Poly(methacrylic anhydride)

Previously, we reported that the glutaric anhydride type polymers, PMA AN and poly(acrylic anhydride), undergo photochemical degradation by decarboxylation, which results in a main chain scission with the formation of olefin and ketene end groups. The evidence for this conclusion was obtained from low-temperature infrared absorption spectroscopy in which the ketene bands, 2125 cm^{-1} for $\text{HC}(=\text{C}=\text{O})\text{CH}_2\sim$ and 2145 cm^{-1} for $\text{CH}_3(=\text{C}=\text{O})\text{CH}_2\sim$, could be identified [13]. However, glutaric anhydrides, the model compounds, yielded mainly cyclobutanones [22]. The low-temperature Fourier transform infrared spectrum of Fig. 11 shows that formation of the ketene end group took place during the electron-beam exposure, but that it underwent further decarbonylation to yield the olefin end group. Larger energies are involved in the electron-beam exposures than in the uv photolysis, and a ketene is known to decarbonylate readily in its excited states [23]. The epr spectrum of PMA AN of Fig. 5 also supports the following degradation mechanism:



The observed epr spectrum is a composite of three radicals: the propagating radical, $\dot{1}$; $(\text{CH}_3)_2\dot{\text{C}}\text{CO}_2\sim$ formed by the hydrogen addition; and RCO [16]. In gamma-ray radiolysis and high-energy electron-beam exposures, the yields of the propagating radicals, under identical dosages, were least from PMA AN in comparison with PMMA and PMA, with relative ratios 0.8:1:2.3, respectively. From the yields of gaseous products, particularly CO_2 , main chain scission in PMA AN is estimated to take place about six times more readily than in PMMA. From these data, the molecular mechanism yielding the ketene end group is concluded to be approximately eight times more efficient than the free radical scission yielding the propagating radical for PMA AN. However, the predominant process for PMMA and PMA is radical main chain scission induced by the removal of the side group. The driving force for main chain scission is allylic stabilization of the propagating radicals. Allylic stabilization may explain why the tertiary isobutyl type macroradicals have never been observed [24]. The epr spectrum of PMA AN, exposed to the gamma-ray and high-energy electron beams at 77 K, is similar to that obtained from PMMA, again except for the methyl and formyl radicals (Figs. 7 and 8). Furthermore, another perturbation of the lines in PMMA is due to direct hydrogen elimination from the methyl ester group. This broadening of the epr lines is due mainly to hydrogen elimination from the methyl group attached to the main chain [25].

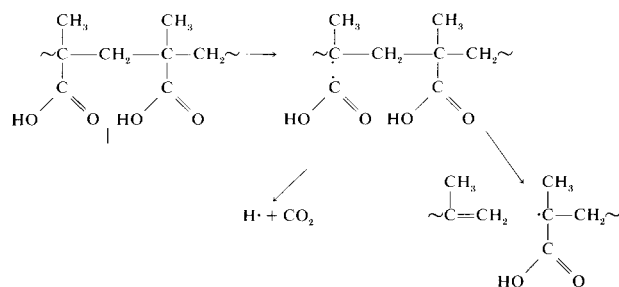
The significant yield of hydrogen under electron-beam exposure may be caused by the same mechanism described for PMMA. Negative hydrogen atoms (see Fig. 2) again play an important role for hydrogen formation. The observed ions CO_2^- (metastable, broad line), O^- , OH^- , H_2O^- , CO^- , and O_2^- clearly indicate electron attachment to the polymer and point out CO_2^- elimination. It is well known that CO_2^- decomposes to O^- and CO because of dissociative electron attachment in the gas phase. The reason for our observation of CO_2^- may be the large quantity of gaseous products present, particularly water, which stabilize the CO_2^- . The O^- is likely to yield water [26]. At this stage we cannot yet differentiate between two alternatives. The electron may attach directly to the polymer to produce CO_2^- , or it may attach to the diradicals shown in the reaction scheme.

• *Poly(methacrylic acid)*

Ormerod and Charlesby [5] reported a single-line epr spectrum with a shoulder for PMA under gamma-ray radiation. Our sample [27] yielded the spectra for gamma-ray and high-energy electron-beam exposures shown in Figs. 7(c) and 8. They closely resemble results obtained in earlier work, except with five percent of the monomer added [5]. We tried to convert our

powder samples to the anhydride structure by simply heating them at 473 K for several hours in a vacuum and removing the monomer by pumping. This treatment, however, yielded only the same spectrum as obtained from PMA in gamma-radiolysis at 77 K, indicating incomplete conversion to the anhydride structure. In uv photolysis at 77 K, PMA yielded a spectrum similar to the one obtained from PMA AN with the intense central peak ascribable to $\dot{\text{C}}\text{OOH}$.

In gamma-ray and high-energy electron-beam exposures of PMA at 77 K, unstable characteristics of $\dot{\text{C}}\text{OOH}$ were responsible for the nearly complete conversion to propagating radicals without $\dot{\text{C}}\text{OOH}$. Relative yields of the propagating radicals at 77 K under electron-beam exposure (600 keV, 10 pulses, 10 J each) were 1.0:2.3:0.8 for PMMA, PMA, and PMA AN, respectively. Combining this result with that of the respective yields of the side group removal, 2.0:7.4:16, we concluded that main chain scission of PMA proceeded in a free radical mechanism induced by side chain elimination, as shown in the following scheme:



Allylic stabilization of the propagating free radicals may be the major driving force of main chain scission. This is in spite of the fact that H^- elimination from the methyl group leading to the main chain scission also takes place, especially with electrons having energies higher than the appearance potential of H^- .

Summary

The radiation chemistry of poly(methacrylates) such as poly(methyl methacrylate), poly(*t*-butyl methacrylate), poly(methacrylic anhydride), and poly(methacrylic acid) has been studied under uv-light, gamma-ray, and electron-beam irradiation. From mass spectroscopic and low-temperature epr and infrared studies, together with analysis of end products, main chain scission induced by side group elimination is considered the common feature of the radiation-induced degradation of all poly(methacrylates). Main chain scission proceeds in a radical mechanism, except for poly(methacrylic anhydride) which undergoes main chain scission mainly in a molecular fashion, yielding the olefin and ketene end groups. The unique feature of electron-beam exposure is the

large yield of hydrogen and negative hydrogen atoms generated either by electron attachment to radicals or by direct elimination of the negative ions.

Acknowledgments

The author thanks J. Bargon and H. E. Hunziker for their help and encouragement during the course of this study; L. W. Welsh, Jr. for his skillful technical help; D. E. Johnson (deceased) and E. Gipstein for their supply of the stereospecific PMMA; and N. Dalal and F. L. Rodgers for their technical help in instrument utilization.

References and notes

1. I. Haller, M. Hatzakis, and R. Srinivasan, *IBM J. Res. Develop.* **12**, 251 (1968).
2. D. L. Spears and H. L. Smith, *Electron. Lett.* **8**, 102 (1972).
3. For instance, M. Dole, *Radiation Chemistry of Macromolecules*, Vol. II, Academic Press, Inc., New York, 1973, p. 97.
4. A. R. Shultz, P. I. Roth, and J. M. Berge, *J. Polymer Sci. (Part A)* **1**, 1651 (1963).
5. H. G. Ormerod and A. Charlesby, *Polymer* **5**, 67 (1964); see also Ref. 6.
6. Excellent reviews of epr studies of PMMA are given in the following: D. Campbell, *J. Polymer Sci. (Part D)* **4**, 91 (1970); K. Tsuji, *Adv. Polymer Sci.* **12**, 131 (1973).
7. A. Todd, *J. Polymer Sci.* **42**, 223 (1960).
8. C. David, D. Fuld, and G. Geuskens, *Makromol. Chem.* **139**, 269 (1970).
9. R. B. Fox, *Progress in Polymer Science*, Vol. I, edited by A. D. Jenkins, Pergamon Press, Inc., New York, 1967, p. 45.
10. P. R. E. J. Cowley and H. W. Melville, *Proc. Roy. Soc., Ser. A* **210**, 461 (1952).
11. J. R. MacCallum and C. K. Schoff, *J. Chem. Soc., Faraday Trans.* **67**, 2372 (1971).
12. A similar technique is reported by J. M. Goodings, J. M. Jones, and D. A. Parks, *Int. J. Mass Spectrom. Ion Phys.* **9**, 417 (1972).
13. H. Hiraoka, *Macromolecules* **9**, 359 (1976).
14. I. S. Ungar, J. F. Kircher, W. B. Gager, F. A. Sliemers, and R. I. Leininger, *J. Polymer Sci. (Part A)* **1**, 277 (1963).
15. A weak fluorescence from PMMA under a nanosecond electron pulse of 10 MeV was reported by S. K. Ho and S. Siegel in *J. Chem. Phys.* **50**, 1142 (1969); their total observation time was about 1000 ns, but long delayed emission was not studied. The delayed emission was probably due to electron recombination to polymer cations and radicals. Continuous bombardment by electrons on one spot rapidly diminishes emission intensity. A similar emission spectrum from hydrocarbons in low-temperature gamma-ray radiolysis was reported by M. Burton, M. Dillon, and R. Rein in *J. Chem. Phys.* **41**, 2228 (1964).
16. Similar spectra have been reported for methyl methacrylate and methacrylic acid in the presence of benzoic peroxide by T. Komatsu, T. Seguchi, H. Kashiwabara, and J. Sohma, *J. Polymer Sci. (Part C)* **16**, 535 (1967).
17. The Norrish type II reaction usually takes place with γ -hydrogen, but few examples are known for β -hydrogen transfer as in the case of PMMA, if it is applicable. For example, see J. G. Calvert and J. N. Pitts, Jr., *Photochemistry*, John Wiley & Sons, Inc., New York, 1967, p. 384.
18. J. H. Richardson, L. M. Stephenson, and J. I. Brauman, *J. Amer. Chem. Soc.* **97**, 2967 (1965); see also their earlier papers referenced herein.
19. Ethyl mercaptan and diphenyl are reported to act as traps for radicals and electrons in PMMA; see Ref. 8, and Ho and Siegel's paper in Ref. 15.
20. J. G. Dillard, *Chem. Reviews* **73**, 589 (1973).
21. L. Kevan and W. F. Libby, *Advances in Photochemistry*, Vol. 2, edited by W. A. Noyes, Jr., G. S. Hammond, and J. N. Pitts, Jr., Interscience Publishers, New York, 1964, p. 183.
22. H. Hiraoka, *J. Amer. Chem. Soc.* **95**, 1664 (1973).
23. See Calvert and Pitts' *Photochemistry*, Ref. 17, p. 392.
24. Kircher et al. reported their observation of the diffused eight-line epr spectrum ascribable to $\sim\text{CH}_2\dot{\text{C}}(\text{CH}_3)\text{CH}_2\sim$, but their identification was not secure; cf. J. F. Kircher, F. A. Sliemers, R. A. Markle, W. B. Gager, and R. I. Leininger, *J. Phys. Chem.* **69**, 189 (1965).
25. The similarity of the epr spectra of PMA AN and PMMA supports the direct hydrogen elimination of the methyl group in PMMA, which is different from the view expressed by G. Geuskens and C. David, *Makromol. Chem.* **165**, 273 (1973).
26. J. D. Craggs, *Advances in Mass Spectrometry*, Vol. 6, edited by A. R. West, Applied Science Publishers, Ltd., Earking, Essex, England, 1974, p. 1.
27. Neither the nmr nor the infrared spectra showed any olefinic protons in our sample.

Received January 30, 1976; revised August 23, 1976

The author is located at the IBM Research Division laboratory, 5600 Cottle Road, San Jose, California 95193.